TR-1166

CALCULATIONS OF RELAXATION OSCILLATIONS IN GAS TUBE CIRCUITS

Alford L. Ward

Larry G. Schneekloth

28 August 1963

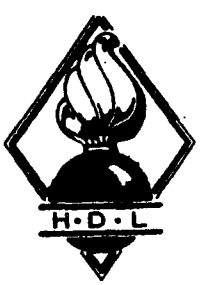

HARRY DIAMOND LABORATORIES
FORMERLY: DIAMOND ORDNANCE FUZE LABORATORIES
ARMY MATERIEL COMMAND
WASHINGTON 25, D.C.

HARRY DIAMOND LABORATORIES

Robert W. McEvoy
LtCol, Ord Corps
Commanding

B. M. Horton
Technical Director

MISSION

The mission of the Harry Diamond Laboratories is:

(1) To perform research and engineering on systems for detecting, locating, and evaluating targets; for accomplishing safing, arming, and munition control functions; and for providing initiation signals: these systems include, but are not limited to, radio and non-radio proximity fuzes, predictor-computer fuzes, electronic timers, electrically-initiated fuzes, and related items.

(2) To perform research and engineering in fluid amplification and fluid-actuated control systems.

(3) To perform research and engineering in instrumentation and measurement in support of the above.

(4) To perform research and engineering in order to achieve maximum immunity of systems to adverse influences, including countermeasures, nuclear radiation, battlefield conditions, and high-altitude and space environments.

(5) To perform research and engineering on materials, components, and subsystems in support of above.

(6) To conduct basic research in the physical sciences in support of the above.

(7) To provide consultative services to other Government agencies when requested.

(8) To carry out special projects lying within installation competence upon approval by the Director of Research and Development, Army Materiel Command.

(9) To maintain a high degree of competence in the application of the physical sciences to the solution of military problems.

UNITED STATES ARMY MATERIEL COMMAND
HARRY DIAMOND LABORATORIES
WASHINGTON 25, D.C.

DA-1A010501B010 TR-1166
AMCMS Code 5011.11.838
HDL Proj. 96600 28 August 1963

CALCULATIONS OF RELAXATION OSCILLATIONS IN GAS TUBE CIRCUITS

Alford L. Ward
Larry G. Schneekloth

FOR THE COMMANDER
Approved by:

for J. H. Van Tuyl
P. E. Landis
Chief, Laboratory 900

CONTENTS

ABSTRACT

Temporal voltage-current dynamic characteristics have been computed using the Townsend continuity equations and Poisson's equation, with suitable initial and boundary conditions. In the current region of the negative static characteristic, small current perturbations initially grow exponentially in time if the external-circuit time constant is greater than the tube current-growth time constant. In a limited range of applied voltages, these oscillations become precisely repetitive in time, corresponding to the well known relaxation oscillations. The frequencies of the oscillations obtained from these calculations agree with those measured at HDL more closely than do those obtained from the traditional published formula. The inductances and the negative resistances calculated from small-amplitude decaying oscillations agree precisely with those calculated using a sinusoidal incremental applied voltage of the same frequency and average current. Qualitative agreement is also obtained with laboratory measurements of these quantities. Relaxation oscillations are also calculated using voltages that closely approximate the peaks of 60-cps applied voltages. Most of the calculations presented are for an argon gap of 1 cm and for a pressure of 2 torr. Experimental data are presented for both argon and hydrogen.

1. INTRODUCTION

The well known phenomenon of relaxation oscillations in cold-cathode gas tubes is of great practical value (ref 1). In most treatments of these oscillations, the gas tube is considered as a perfect switch, which closes to discharge a condenser from the tube breakdown voltage to its extinction voltage and then opens in zero time. This simplified theory may lead to large errors in calculating the frequency of the relaxation oscillations (ref 2). This report gives a fuller treatment of a paper presented at the 1962 summer meeting of the American Physical Society (ref 3), which for the first time presented a rigorous calculation of the processes within the gas tube in a relaxation oscillator circuit.

2. CALCULATIONS

2.1 Model

The model and resulting formulation used in the calculations, now adapted for the IBM 7090, have been presented previously (ref 4,5). In brief, the Townsend continuity equations for gas ionization are solved simultaneously with Poisson's equation to account for space charge effects. The computer output includes the variation of the tube current and voltage with time. The boundary conditions on the gas tube are imposed by a series resistance R_s and a parallel capacitor C, with a voltage supply which permits either a step voltage or an incremental sinusoidal voltage to be added to the constant d-c supply. The initial conditions are arbitrary, but a stationary state is generally used.

2.2 Approximations

The frequency of relaxation oscillations has been routinely calculated as the reciprocal of the time required for the condenser to charge through the series resistance from the extinction voltage V_x of the tube to the breakdown voltage V_b. This time is readily calculated as

$$T = R_s C \ln [(V_a - V_x)/(V_a - V_b)] \qquad (1)$$

where V_a is the applied voltage. This equation gives no information on the range of values of V_a, R_s, or C for which oscillations occur, or on the currents involved.

A criterion for the stability of the gas tube has been given by Kaufmann (ref 6). The following analysis was made independently but is similar to that of Kaufmann. It has been found (ref 5) that the impedance properties of a gas discharge may be approximated by an inductance, L, and a differential resistance, R. The effective circuit is shown in figure 1.

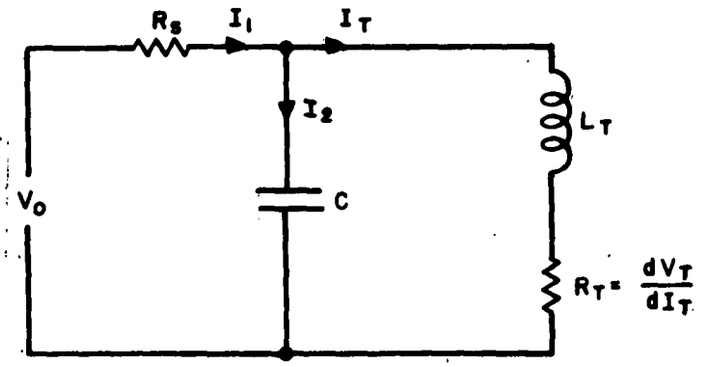

Figure 1. Effective circuit used to analyze gas tube oscillations. The tube is represented as an inductance and an a-c resistance.

Let the steady-state tube current be I_s and the current at any time be I(t). Then the differential equation for the difference current, $i(t) = I(t) - I_s$ is given by

$$\frac{d^2i}{dt^2} + \left(\frac{R}{L} + \frac{1}{R_sC}\right)\frac{di}{dt} + \left(1 + \frac{R}{R_s}\right)\frac{i}{LC} = 0 \qquad (2)$$

The derivation of this equation and its solution is given in the appendix. One form of the solution is

$$i(t) = i(0)\exp(\lambda t)\sin(\omega t + \Phi) \qquad (3)$$

where $\lambda = -\frac{1}{2}\left[\frac{R}{L} + \frac{1}{R_sC}\right]$ and $\omega^2 = \left(1 + \frac{R}{R_s}\right)\frac{1}{LC} - \lambda^2$

From equations (2) and (3) it is seen that if R, the slope of the static characteristic, is positive, the tube is stable for small perturbations. However, if R is negative and of greater magnitude than R_s, the tube is unstable. This instability corresponds to the breakdown of the tube into the glow discharge mode. If R is negative and: (1) if the internal time constant of the tube L/R equals in magnitude the external circuit time constant R_sC, then $\lambda = 0$ and the tube oscillates with a constant amplitude, with the frequency given by the angular frequency, ω; (2) if L/-R is greater than R_sC, then any perturbation in the tube current dies out exponentially; (3) if L/-R is less than R_sC, then λ, the current growth constant, is positive and any perturbation will initially grow exponentially in time. However, both R and L are functions of the tube current, R becoming large and positive in the abnormal glow.

Equations (3) may be solved for R and L to obtain

$$L = -\frac{CR_s}{1 + 2R_sC\lambda}R \qquad R = \frac{-R_s(1 + 2R_sC\lambda)}{1 + 2R_sC\lambda + R_s^2C^2(\omega^2 + \lambda^2)} \qquad (4)$$

3. EXPERIMENTAL MEASUREMENTS

Experimental measurements for relaxation oscillations have been reported in reference 2. The present paper reports more extensive work and analysis completed at HDL since that report. The experimental arrangement is shown in figure 2 (next page). Data were obtained using two different experimental parallel-plate tubes. One tube contained argon gas at a pressure of 9 torr with nickel electrodes spaced 0.84

cm apart. The second tube was built with a nickel cathode, with the possibility of varying both the filling gas pressure and the electrode spacing.

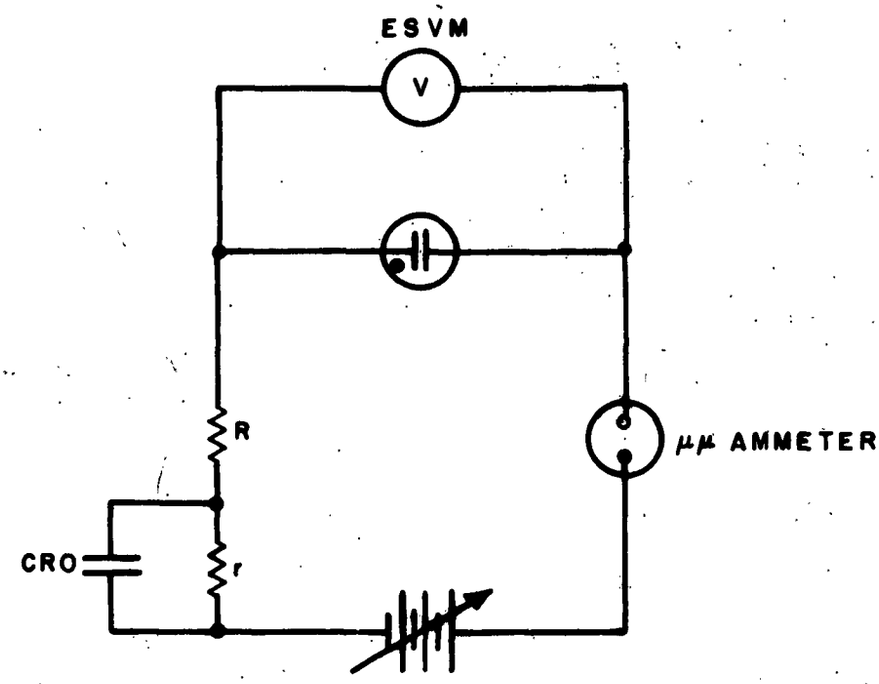

Figure 2. Schematic circuit of experimental apparatus used to measure tube oscillations.

Relaxation-type oscillations were observed and studied in the course of obtaining the static characteristic curve in a current range from 10^{-6} to 10^{-3} amp, which includes the negative slope region of the curve.

4. RESULTS

4.1 Calculations

Most of the calculations have been made for argon at a pressure p of 2 torr, a gap distance d of 1 cm, and a secondary ionization coefficient γ equal to 0.04. The variation of the primary ionization coefficient, the ion and electron mobility with the field E, is given in reference 4.

An example of the buildup of oscillations from a small perturbation is shown in figure 3. After a varying number of oscillations, the oscillations become precisely repetitive in time. Using $R_s = 10^8$ ohms, $C = 3 \times 10^{-9}$ f, a discharge area $s = 10$ cm^2, and an externally produced current, $J_o = 2 \times 10^{-9}$ amp/cm, relaxation oscillations were found to occur with applied voltages of 173.5 to 180.5 v. At both 173.4 and 181 v the oscillations die out. To define the boundary values more closely would take excessive computer time. The variation of both tube current and voltage with time is shown in figure 4, while a plot of tube voltage versus current is given in figure 5. It will be noted that the frequency of oscillations increases with applied voltage. The variation of frequency with applied voltage is given in figure 6 (a), together with that predicated by equation (1). It is seen that the frequency calculated from equation (1) is about 5 to 6 times that calculated from the computer data. Measurements reported in reference 2 indicated that equation (1) gives frequencies about 3 times greater than those measured under somewhat different experimental conditions. A plot of frequency versus the time average of tube current is given in figure 6 (b), on a log-log plot. The points corresponding to the relaxation oscillations drop slightly below the straight line formed by points obtained outside this region. If J_o is reduced, the frequency of the lower applied voltage oscillations drops sharply, requiring excessive computer time. At higher applied voltages, the current does not reach as low a minimum value and the J_o value has less effect. In fact this higher minimum current is effective in lowering the breakdown voltage in the same way as is J_o. Since the tube breaks down at a lower potential, less charge is stored in the capacitor and consequently the current peak is not so large. This may be noted in figures 3 and 4. The static characteristic calculated from runs of other types is shown in figure 5. It is seen that the static characteristic separates the region where current increases with time and that where current decreases with time. It may also be noted that the load line crosses the dynamic paths at the maximum and the minimum voltages. The time average currents and voltages of the relaxation oscillations are plotted as individual points in figure 5.

The buildup or decay times of the relaxation-type oscillations and their frequency may be used to compute the tube inductance L, and a-c resistance R, by means of equation (4). An alternative method of determining L and R by forced oscillations of an applied frequency F, was presented in reference 4. The good agreement of the inductances calculated by the two methods is presented in figure 7, where the LI product is plotted against the current density. The frequency for the forced oscillations is 1×10^4 cps, while the self-oscillations vary somewhat from that figure. The "no space charge approximation" is discussed in reference 4. The minimal value of the LI product is attained at a current density about 125 percent of the normal current density.

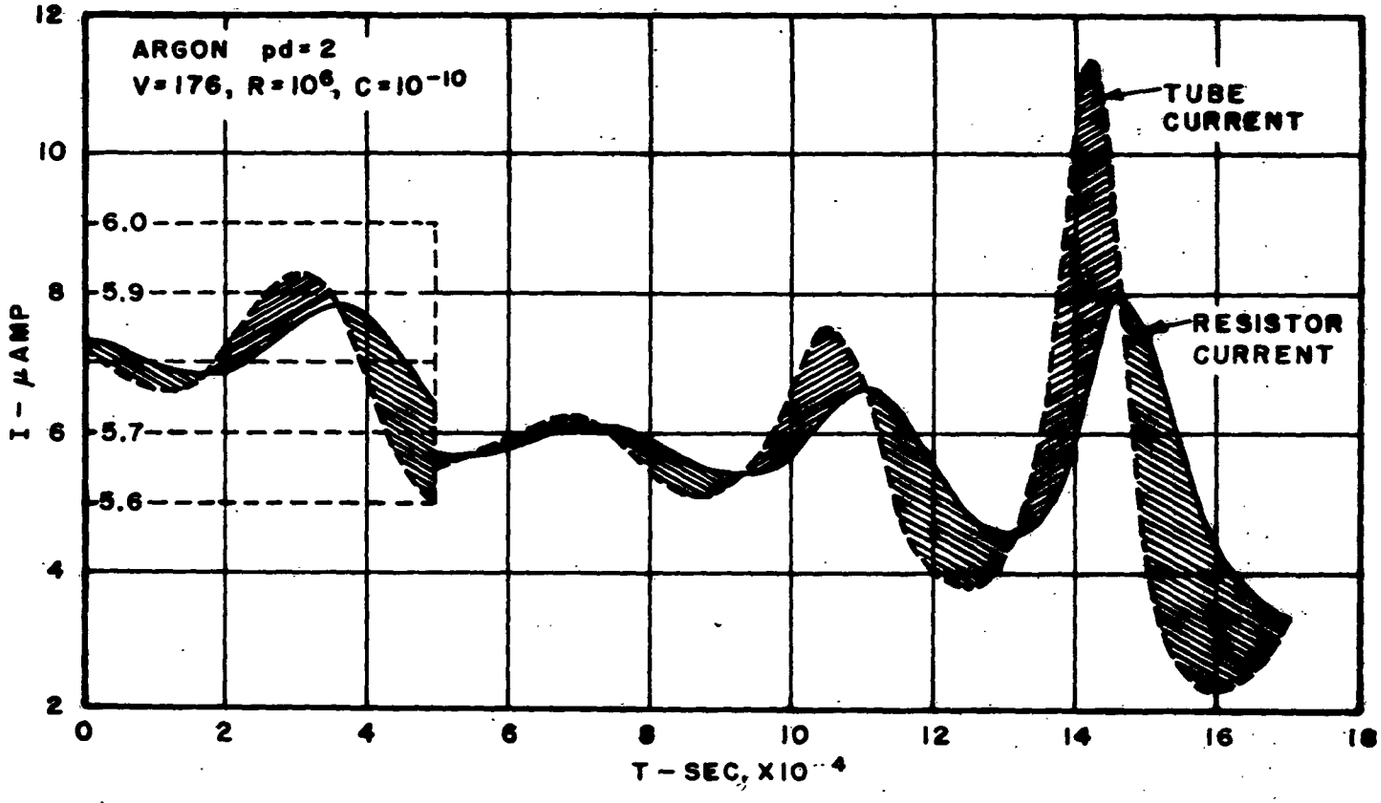

Figure 3. Buildup of oscillations from a small perturbation calculated for an argon tube operating in the negative resistance region.

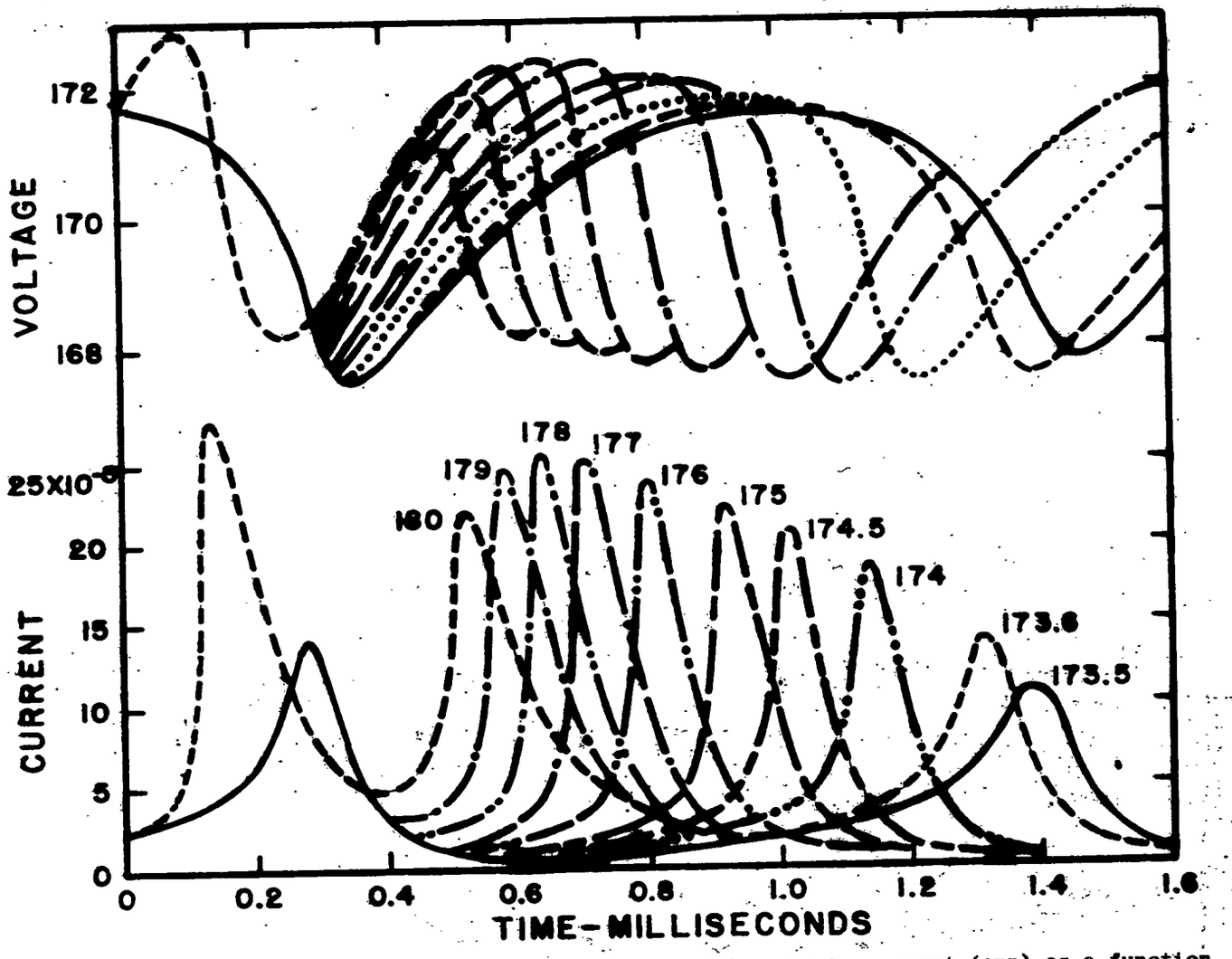

Figure 4. Calculated variation of tube voltage (v) and tube current (amp) as a function of applied voltage, shown as parameter for current curves.

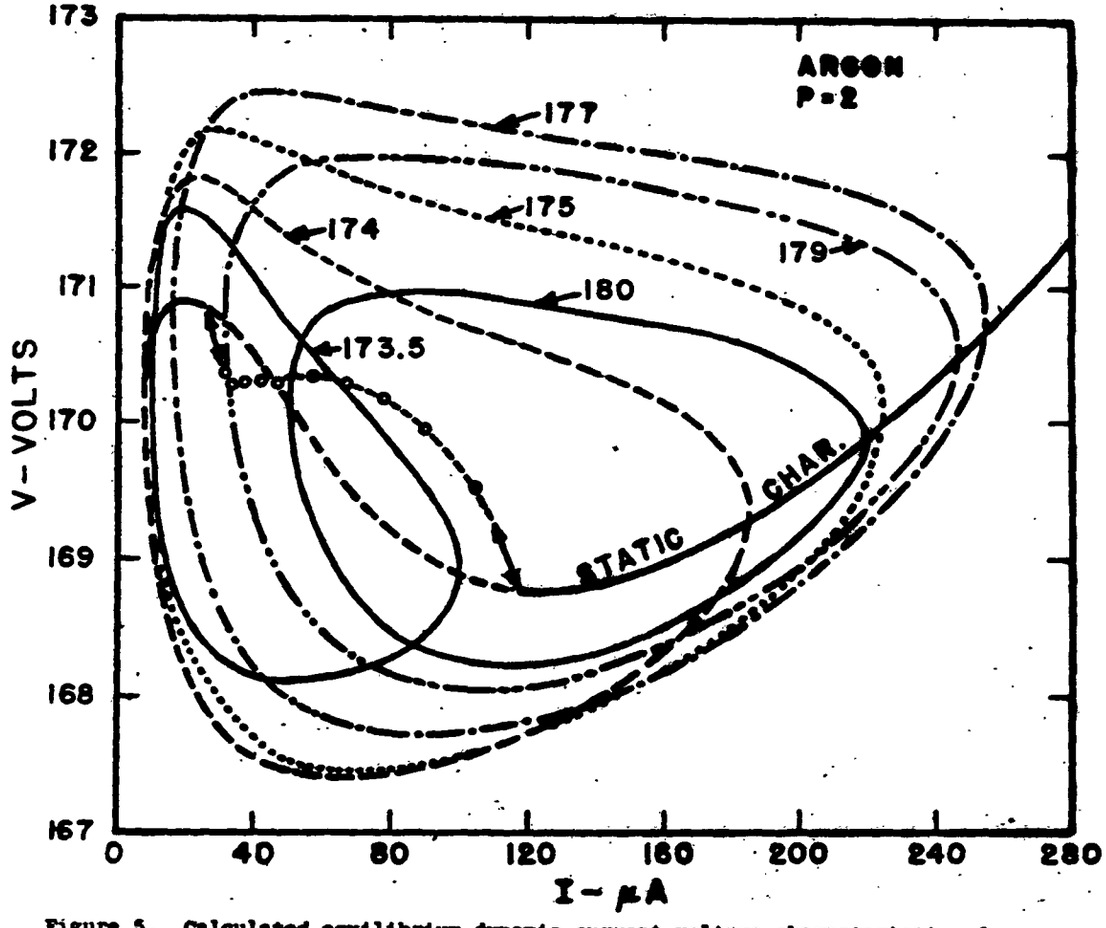

Figure 5. Calculated equilibrium dynamic current-voltage characteristics for relaxation oscillations for various applied voltages. The calculated static characteristic is shown as a solid curve in the stable region and as a dashed curve in the region of oscillations. Individual points indicate calculated time averages of voltage and currents of oscillations.

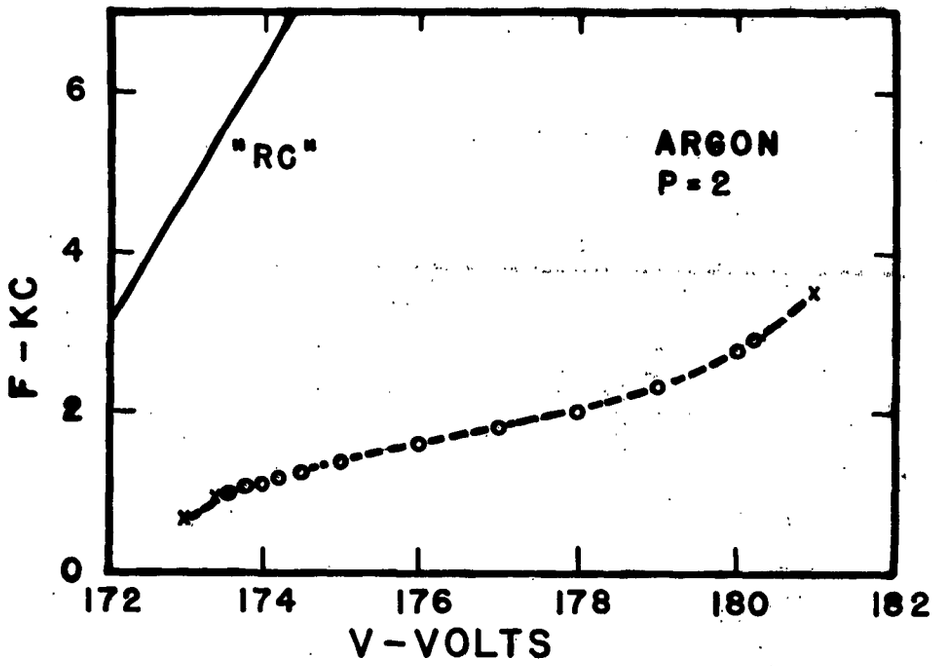

(a) Calculated variation of frequency with applied voltage. Curve marked "RC" is obtained from equation 1. Results obtained for stable relaxation oscillations are shown by open points, while decaying oscillation frequencies are shown by crosses.

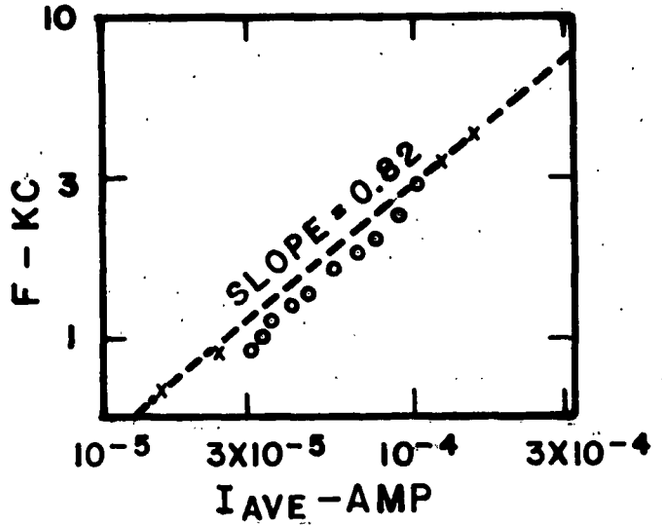

(b) Calculated variation of frequency against average current. Open points represent stable oscillations while crosses indicate decaying oscillations.

Figure 6. Frequency as a function of applied voltage and current.

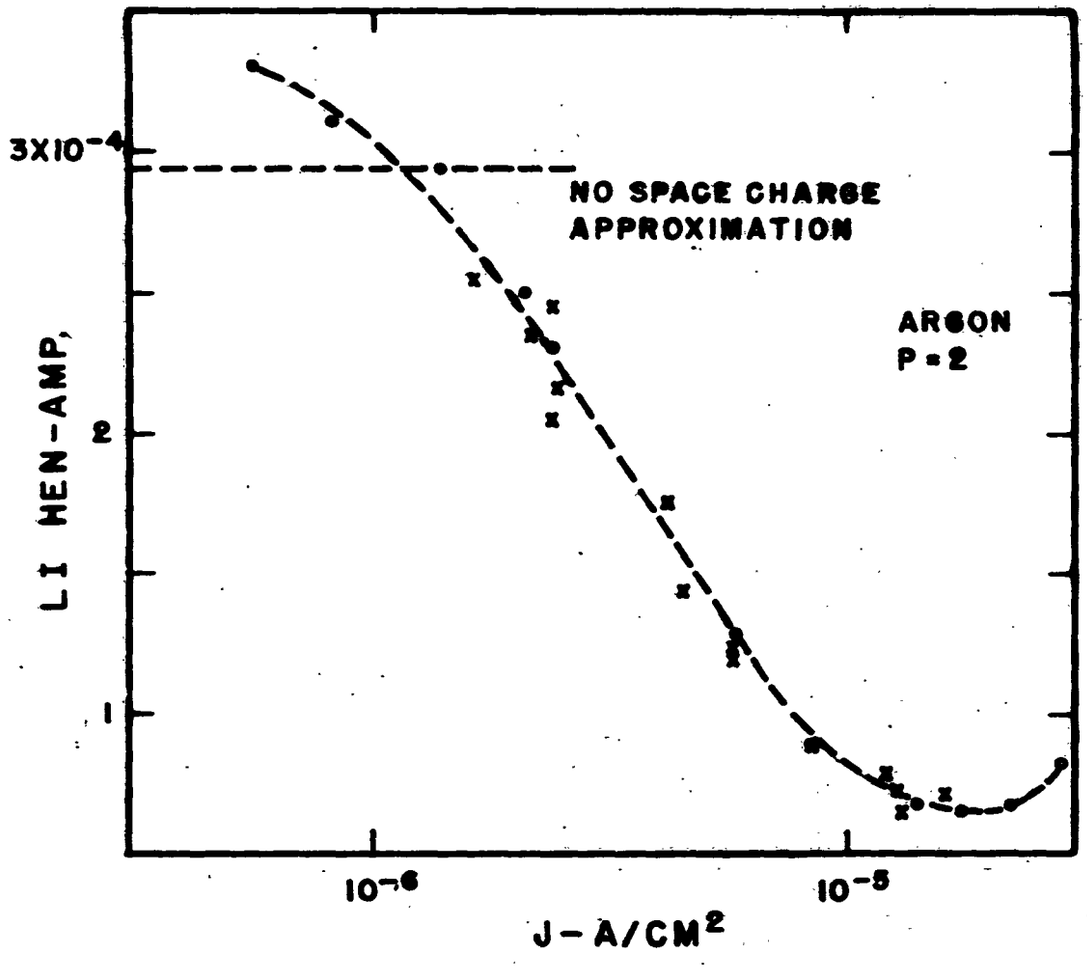

Figure 7. Calculated variation of inductance-current product as a function of the current density. Forced oscillations are given by the open points, while self-oscillations are indicated by crosses.

The variation of impedance and the phase angle (phase lag of the current from the voltage) with frequency is shown in figure 8 for two current densities, 14.0 μa cm^2 (approximately the normal current density) and 17.4 μa/cm^2. It is noted that phase angle reaches a maximum at roughly half the frequency at which the impedance attains its maximum.

The variation of the LI product with frequency is shown in figure 9 for currents in the subnormal glow, the normal glow, and the abnormal glow. Note that the maximum shifts to higher frequencies as tube current increases. A plot of ωLIp versus RIp is given in figure 10. Experimental plots of ωL versus R have generally given semicircular curves. Figure 10 shows that the similarity laws are obeyed over the limited range of current and pressure tested.

It has been found that the portion of the 60-cps a-c voltage above the breakdown voltage may be closely approximated by calculations using an approach voltage and an incremental sinusoidal voltage of appropriate amplitude and frequency. Figures 11 and 12 show the results of a sequence of such calculations simulating 60-cps a-c voltages of the various amplitudes noted. Aside from the applied voltage, the circuit and tube parameters are the same as those used in the previous figures. The top portions of each figure show the applied voltage and the tube voltage as a function of time. The middle figures present the tube and external resistor current as a function of time. The lower figures give the dynamic voltage-current path and the static characteristic. It should be noted that the number of pulses increases with increasing voltage, that a pulse is nearly full size if it exceeds the "breakdown current," and that successive current pulses are smaller than the initial breakdown pulse. Closer scrutiny reveals that the frequency is greater at higher applied voltages. When the load line crosses the static characteristic in the abnormal glow region, the oscillations rapidly die out. The current dies out without oscillations building up as the applied voltage decreases to below the breakdown value. At the two highest applied voltages, calculations were extended only to approximately the maximum voltages, since otherwise the computer time would be excessive.

4.2 Experimental

Current-voltage characteristics were obtained using d-c meters. Therefore, when oscillations are observed on the oscilloscope, the current-voltage points must be considered as representing "average" readings. Such a characteristic is shown in figure 13, where the oscillatory regions are noted on the graph.

Figure 14 shows the variation of the frequency of relaxation oscillations in argon as a function of the "average" current. The data were taken at a pressure of 9 torr and a spacing of 0.84 cm. The effect of the circuit shunt capacitance on the frequency of oscillation is illustrated here. One of these curves has been replotted in figure 15 against applied voltage, and compared with that curve predicted by

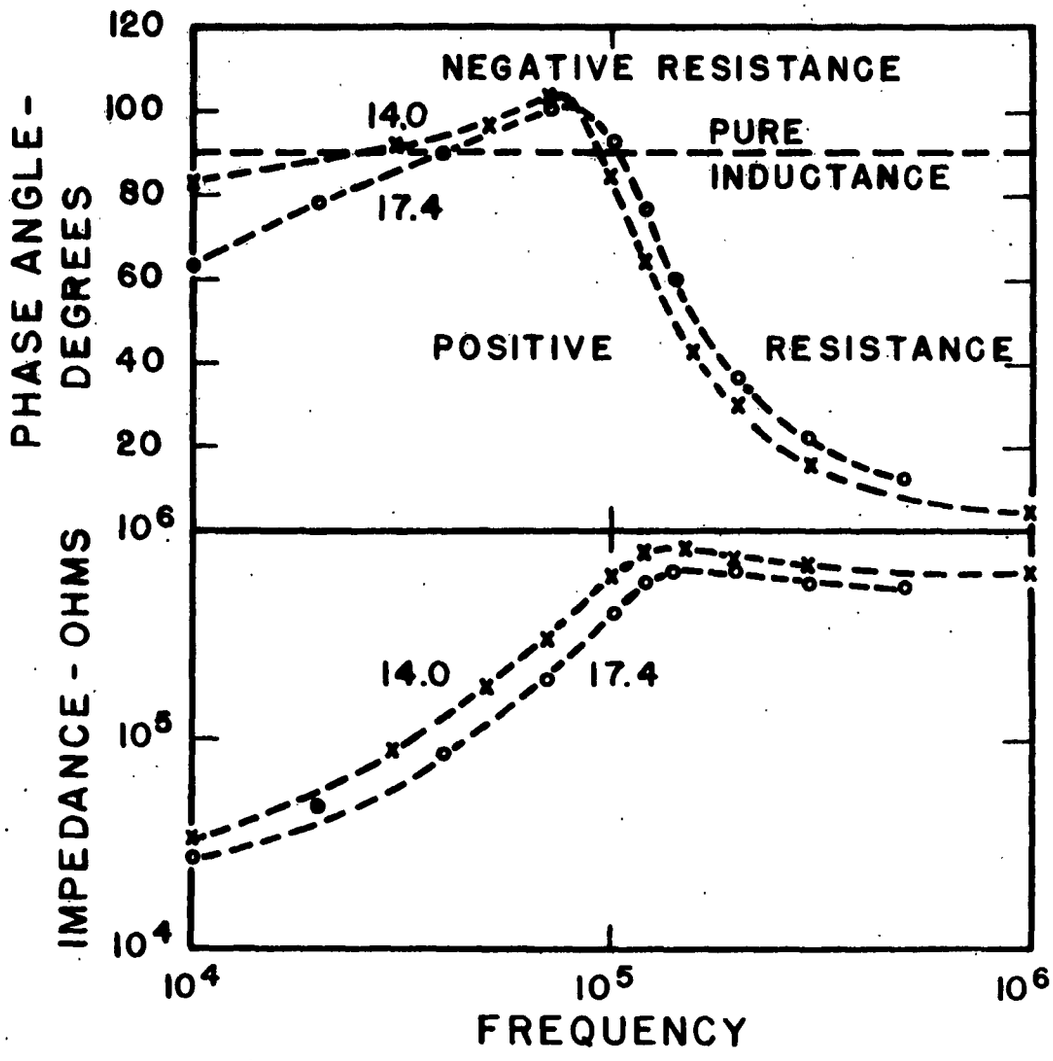

Figure 8. Calculated variation of impedance (lower curves) and phase angle (upper curves) for forced oscillations as a function of frequency in cps for two values of average current density shown in $\mu a/cm^2$.

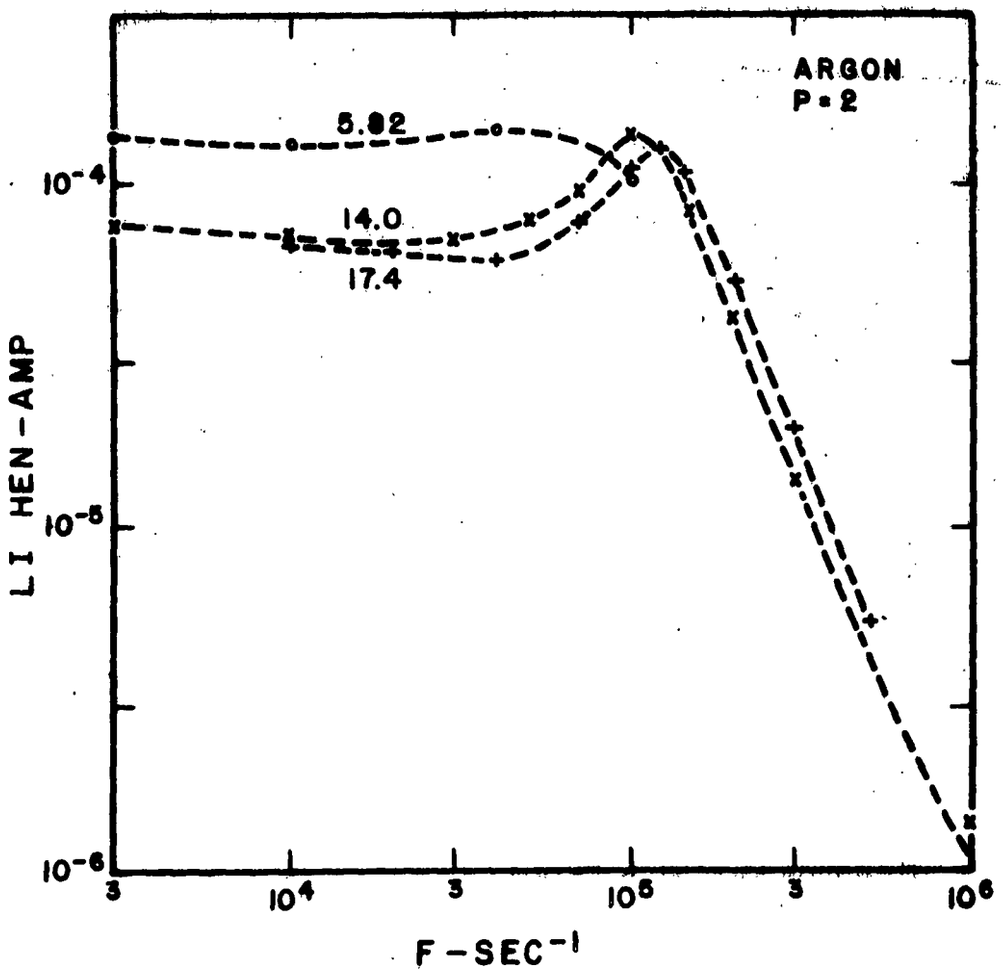

Figure 9. Calculated variation of inductance-current product as a function of the frequency of forced oscillations for three values of average current density shown in $\mu a/cm^2$.

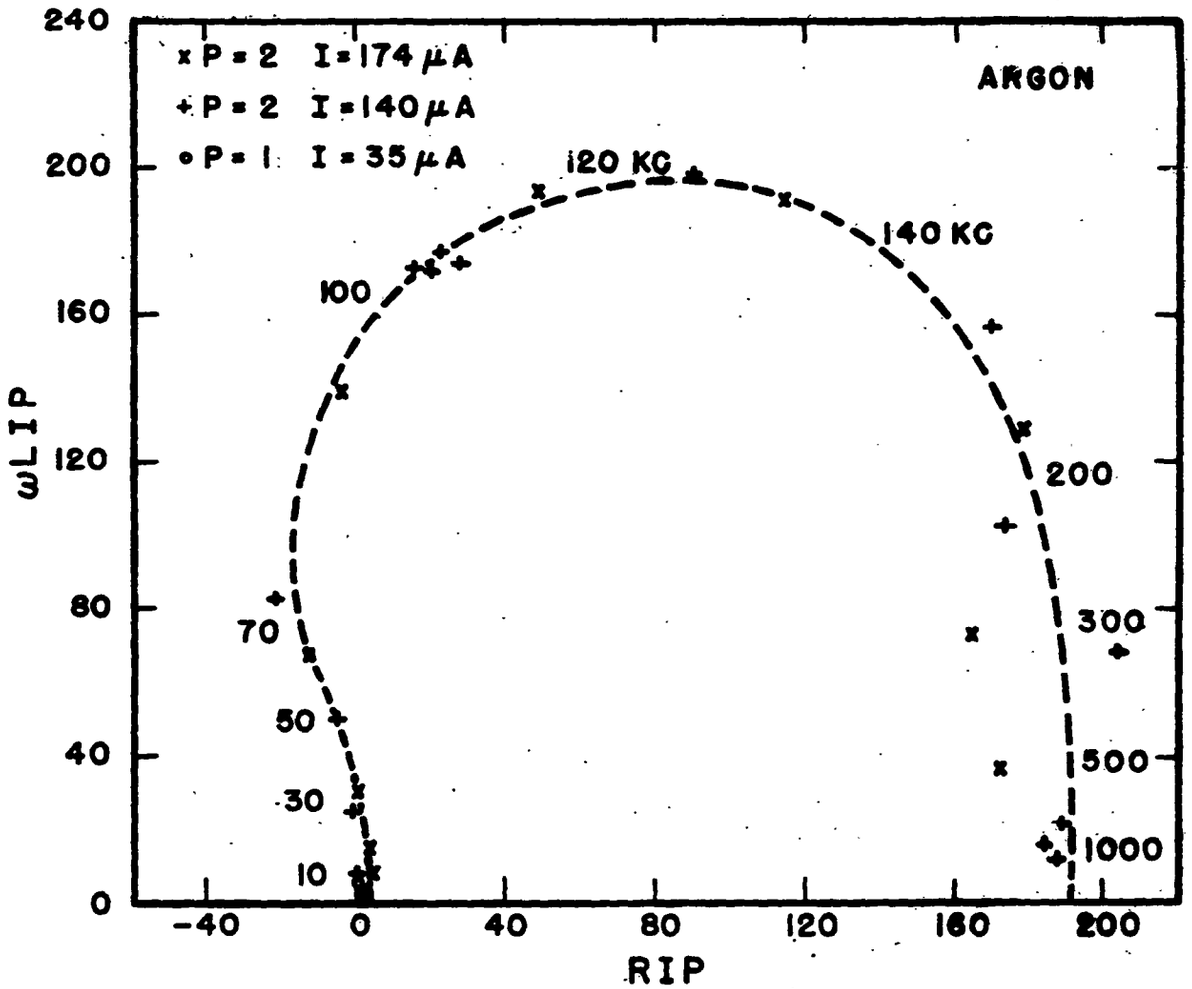

Figure 10. Calculated variation of reactance-current-pressure product with resistance-current-pressure product. Parameter is the applied frequency.

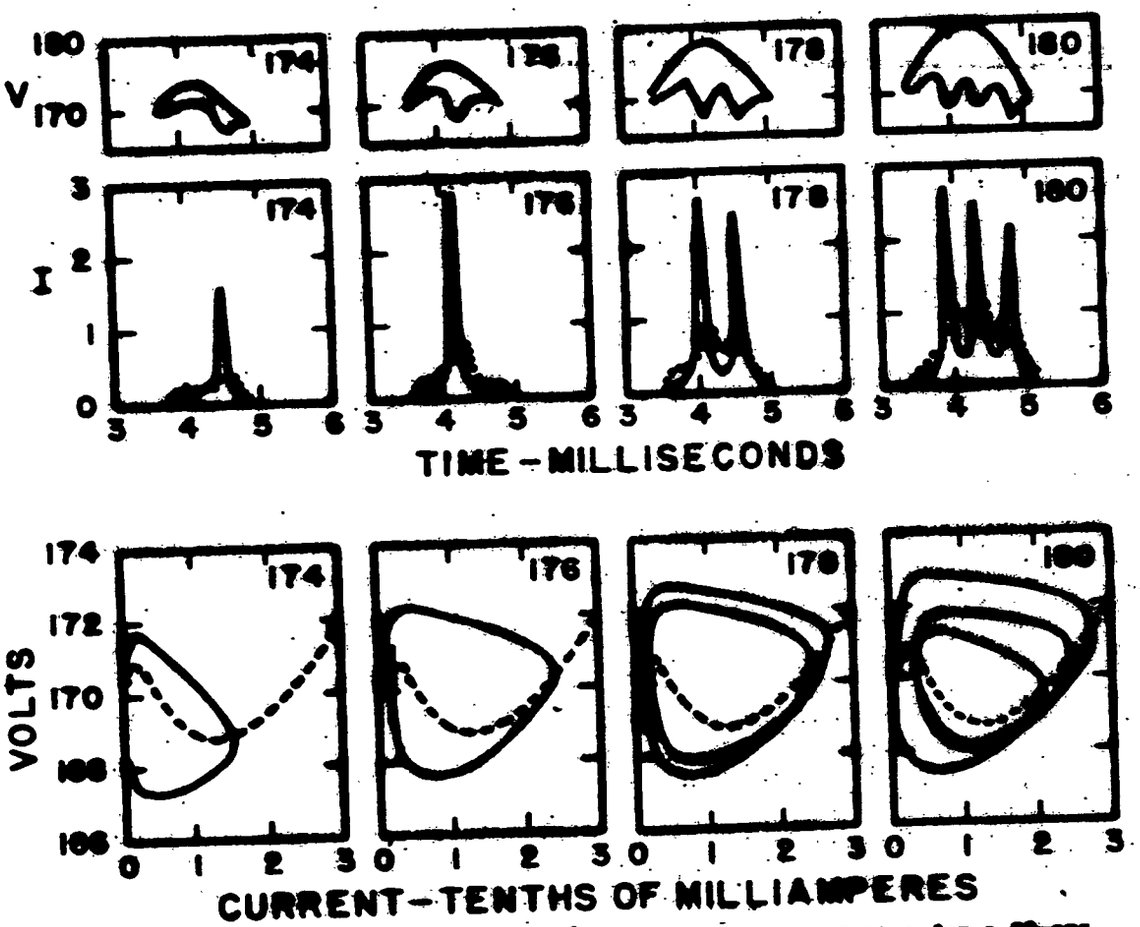

Figure 11. Calculated current and voltage as a function of time for a 60-cps applied voltage. The upper plots show the applied and tube voltages as a function of time for the various maximum applied voltages shown. The center plots show the tube (solid lines) and external circuit (dotted lines) currents as a function of time. The lower curves give the dynamic current-voltage loops (solid lines) and the static characteristics (dashed lines).

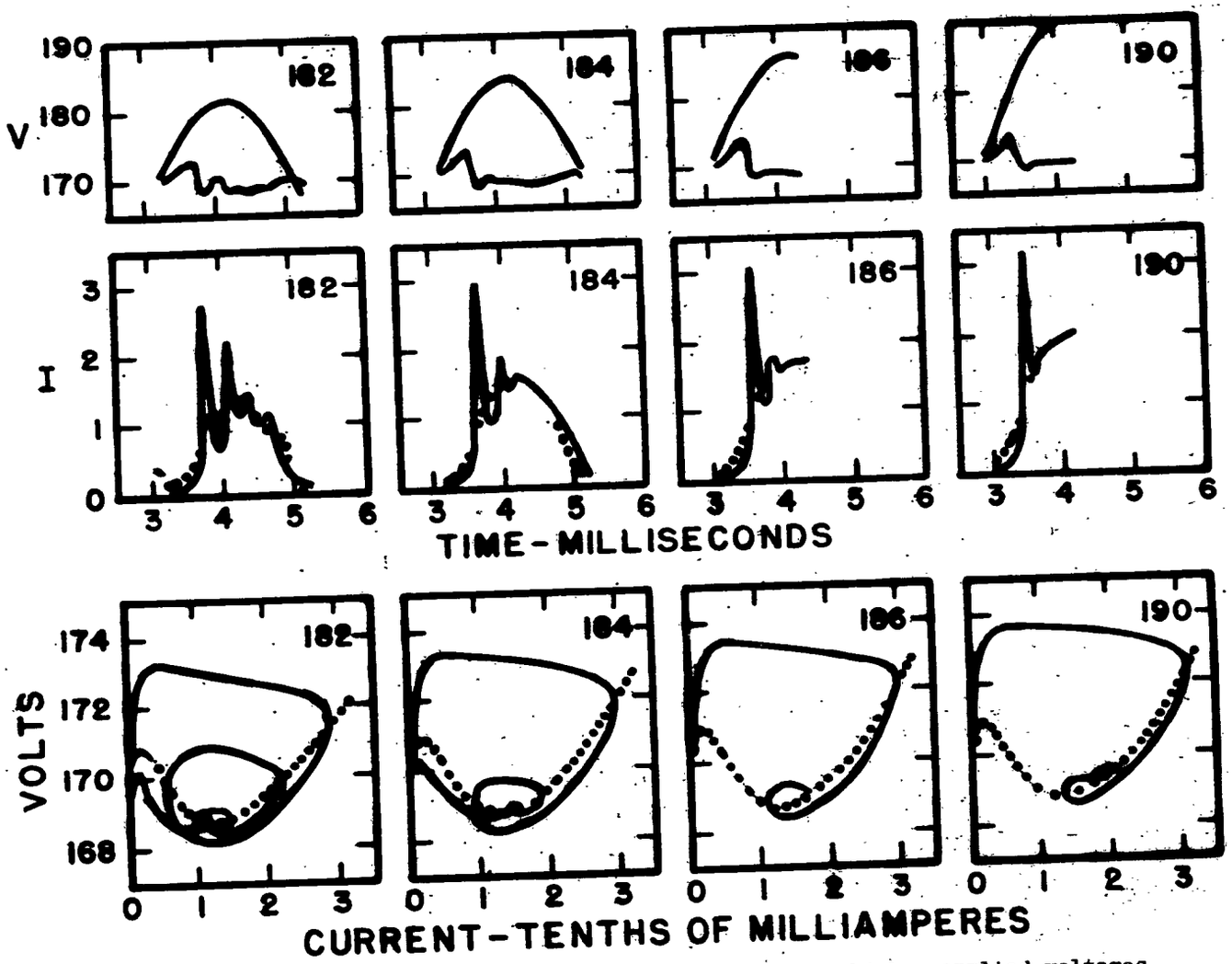

Figure 12. Continuation of information of figure 11 to higher applied voltages.

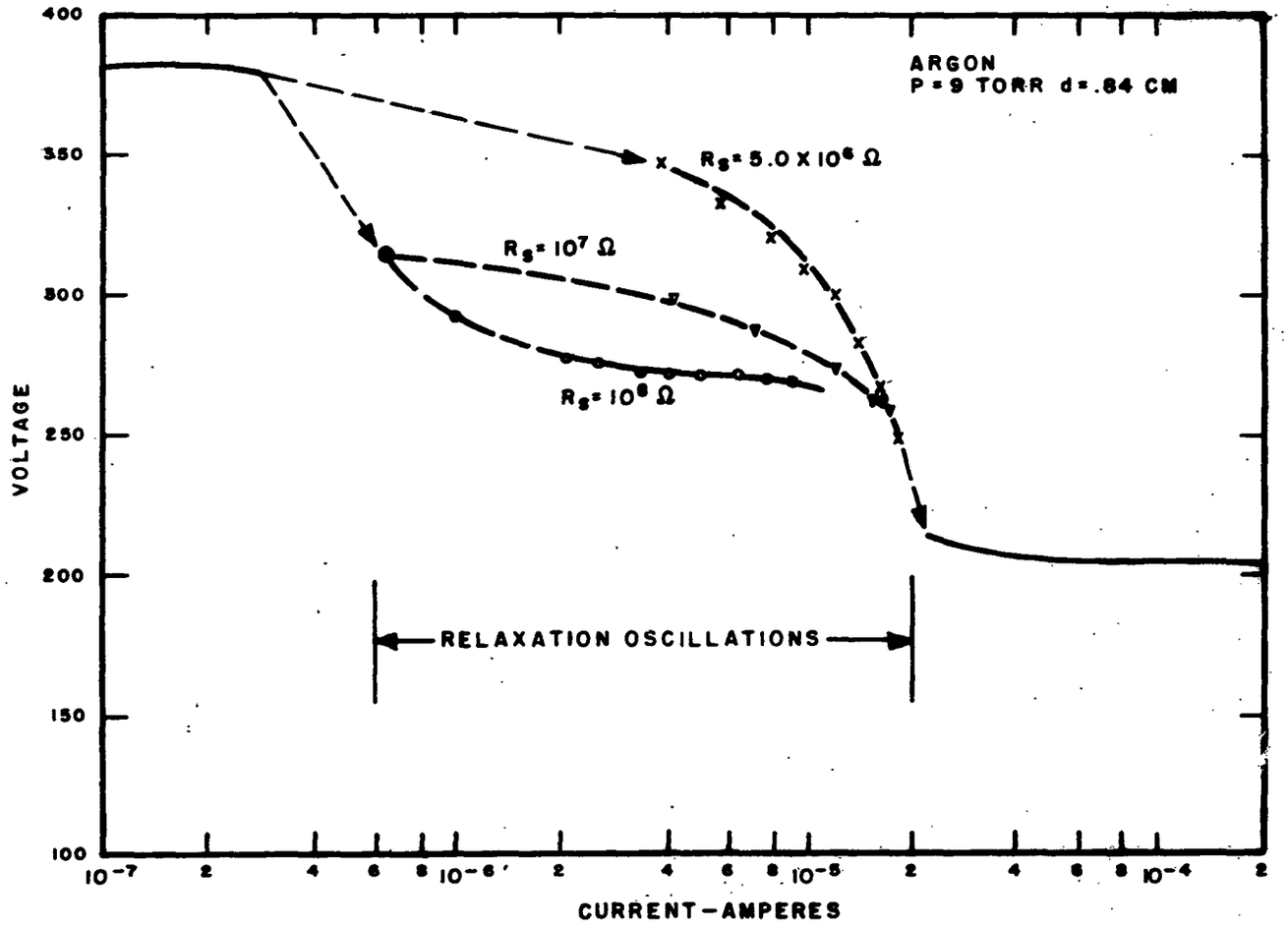

Figure 13. Measured static characteristic (solid curve) and average current and voltage reading (points) for region of relaxation oscillations.

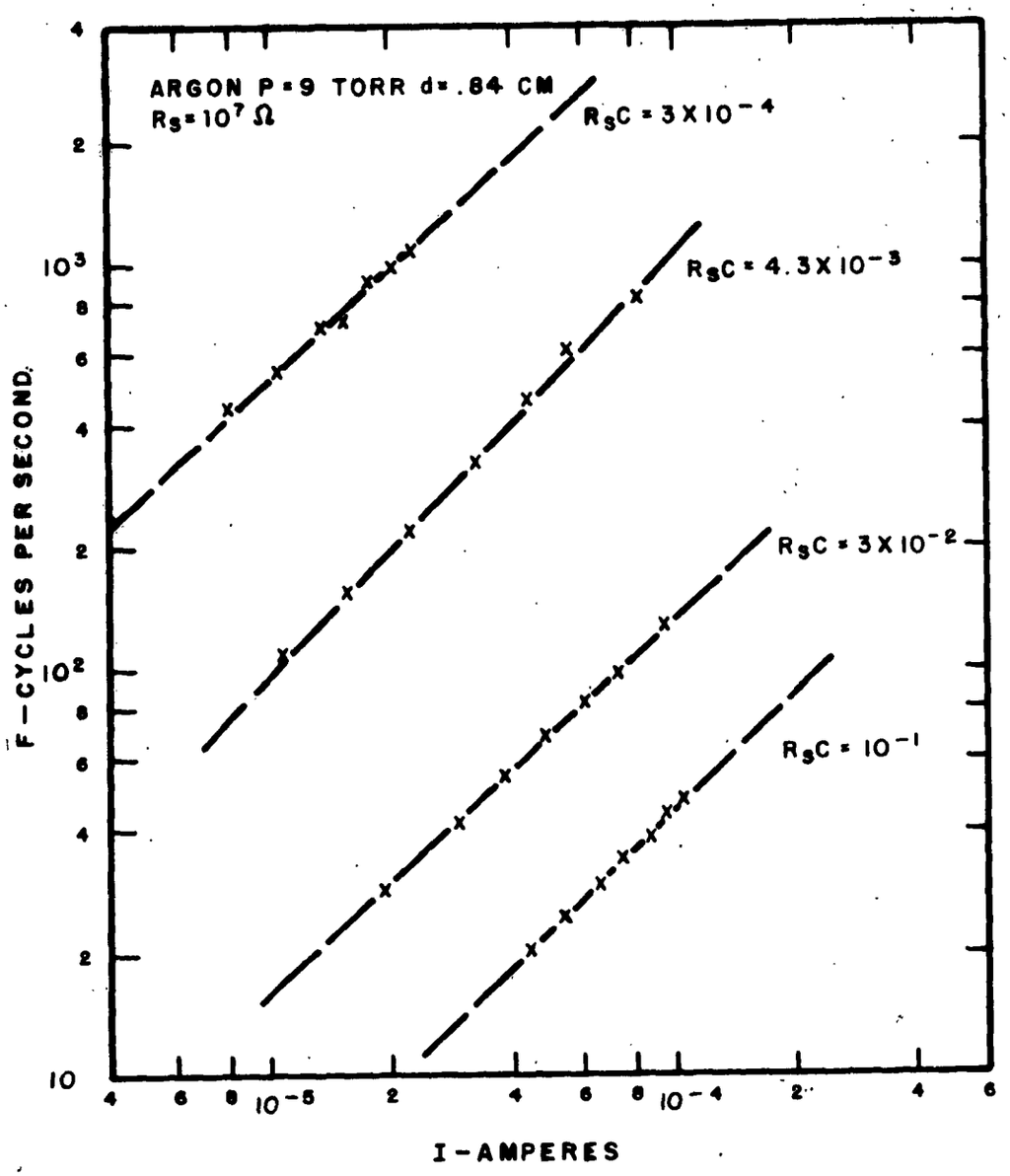

Figure 14. Measured variation of frequency of relaxation oscillations as a function of the average current for a series resistance of 10 meghoms and various values of shunt capacitances.

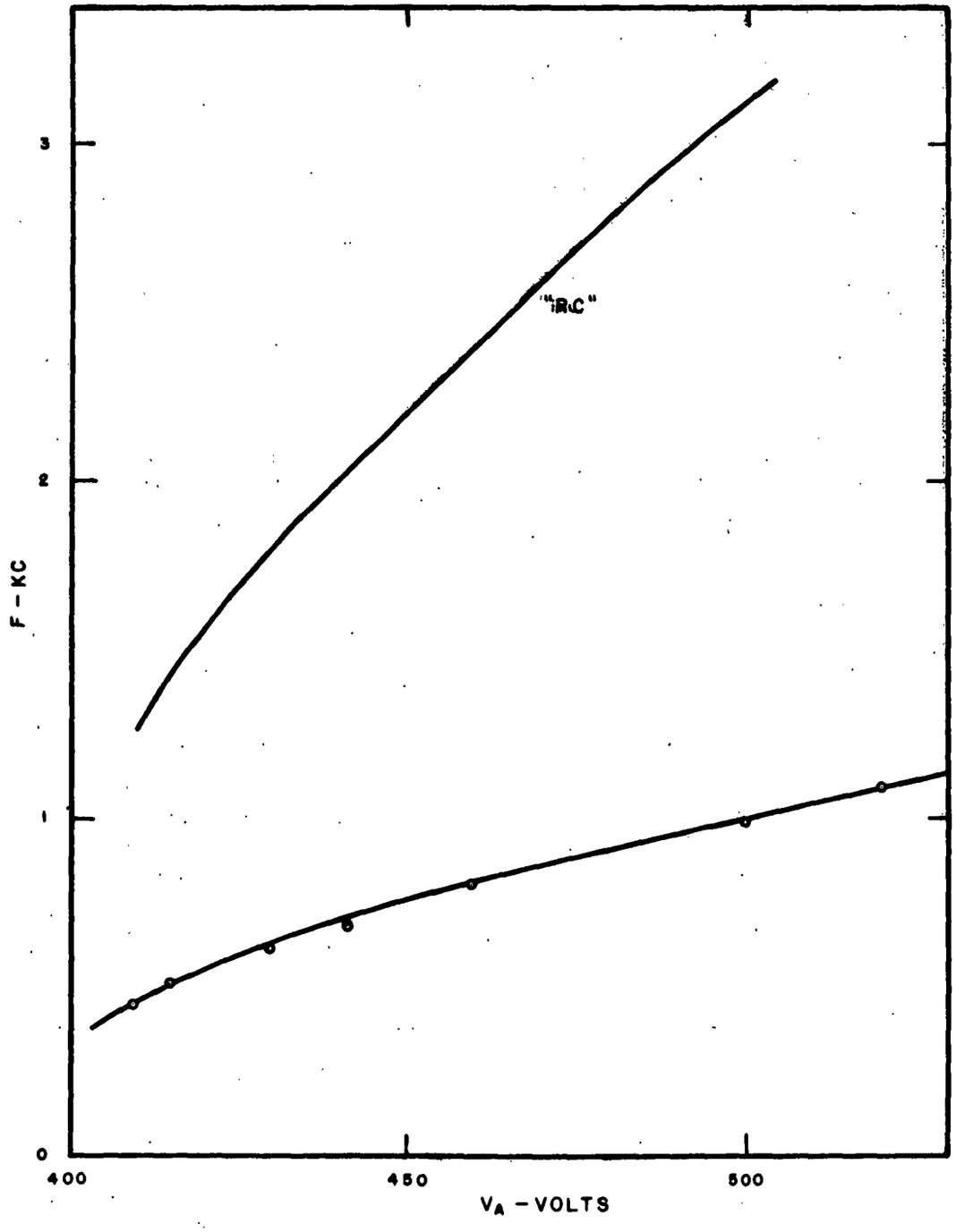

Figure 15. Variation of frequency of oscillations with applied voltage. Curve labeled "RC" was calculated using equation 1, while points show measured values.

equation (1). Note that the frequency of the predicted "RC" curve is 3 to 4 times that of the actual experimental data.

Similar measurements made in hydrogen with a pressure of 2.2 torr and a gap distance of 1 cm are shown in figure 16. This graph plots frequency against current and shows frequency as a function of both series resistance and shunting capacitance.

To correlate the data taken in argon with that in hydrogen, the information from the previous figures has been replotted together in figure 17, where the frequency-pressure product has been plotted against current.

Experimental work has also been done with a 60-cps voltage applied to the tube to compare with similar computer calculations reported above. Examples of oscilloscope traces of this work are photographed in figure 18. This series of pictures was taken with argon at a pressure of 9 torr and a gap distance of 0.84 cm.

Experimental work on the impedance porperties of gas discharges has been reported previously (ref 5).

5. DISCUSSION

The traditional model for calculating the frequency of relaxation oscillations in gas tube circuits assumes that the tube breaks down at a fixed breakdown voltage and extinguishes at a fixed voltage (the normal glow voltage) in a time negligible compared with the time for the condenser to recharge. The frequency may then be calculated by equation (1). It was shown in reference 2, and is further substantiated in this report, that the frequencies thus calculated are larger, by a factor of about 3 or 4, than those measured experimentally at low pressures. An examination of figures 4 and 5 shows that the error may stem from three sources. First, the breakdown voltage is not constant but depends upon both the approach current and the rate of voltage rise. It is normally considerably higher than the breakdown voltage as measured quasi-statically. Likewise, the extinction voltage is not constant but is considerably below the normal glow voltage. Normally, the higher the breakdown voltage, the larger the current spike and the lower the extinction voltage. Finally, the time for the breakdown cannot be neglected at low pressure.

Certain limitations of the calculations and of the ability to make measurements under ideal conditions prohibit direct comparison of the two results. First, the calculations are one-dimensional while the discharge is not. Some success has been achieved in measuring cross-sectional area in static discharges, and this information is of some value in interpreting dynamic measurements. Second, the calculations are, at present, limited to a constant secondary ionization coefficient γ, independent of the cathode field and of the current flowing. It is generally accepted that these factors cause

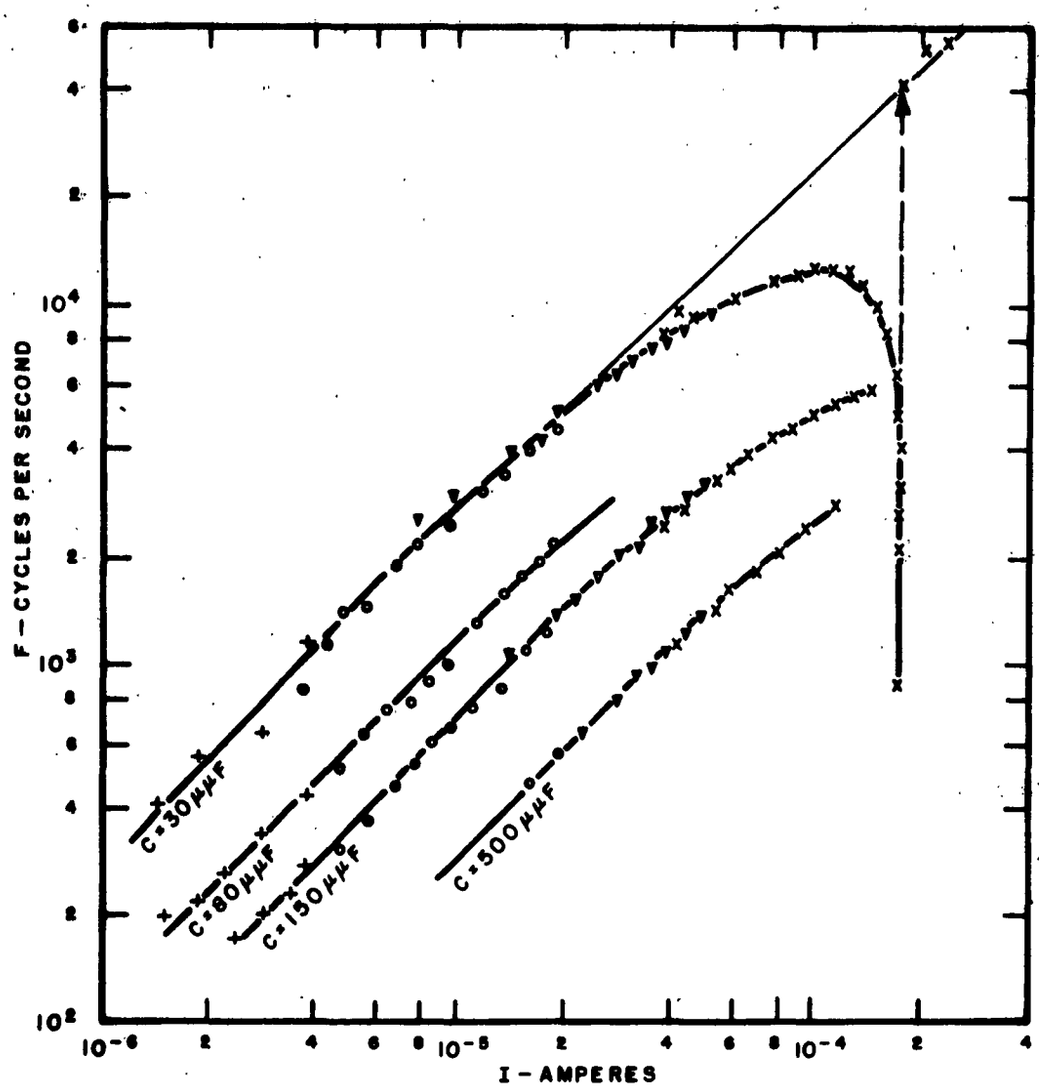

Figure 16. Measured variation of frequency with average current in H_2 gap at a pressure of 2.2 torr. Series resistance values in megohms are given by the following symbols: crosses -1, circles - 10, triangles 4, and plus signs - 50.

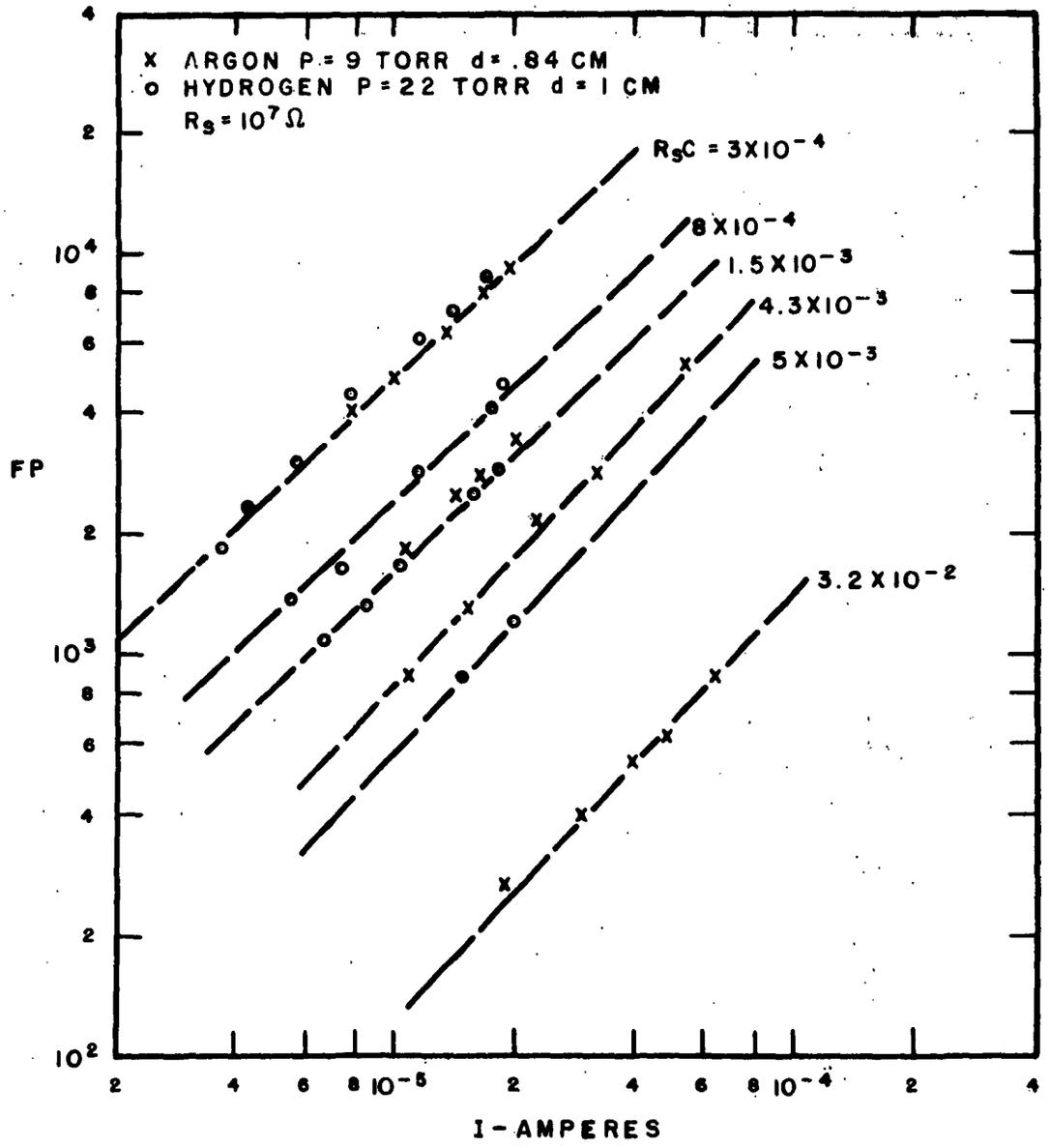

Figure 17. Measured frequency-pressure product as a function of average current for both argon and hydrogen.

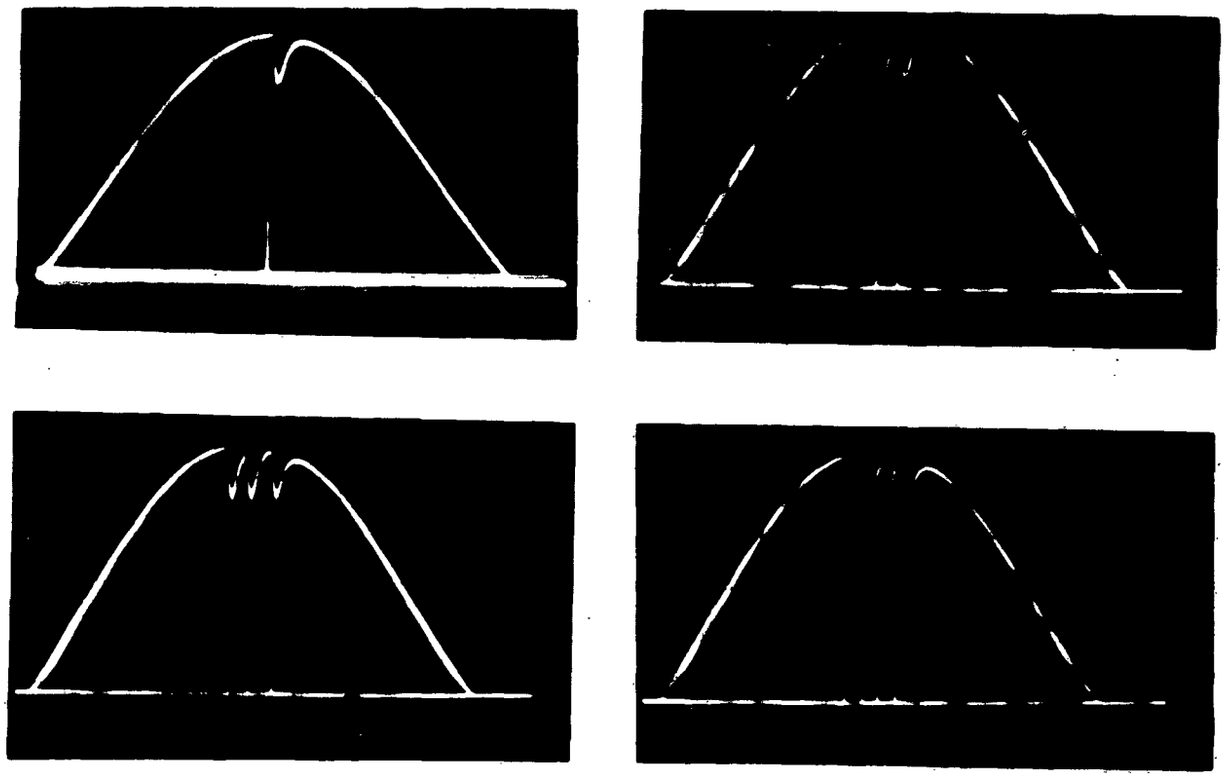

1383-62

Figure 18 . Photographs of relaxation oscillations occurring with 60 cps applied voltage. Both current and voltage traces are shown in each photograph. Successively increased number of oscillations are observed at increasing applied voltages.

large changes in γ at low pressures. Moreover, the calculations have assumed that γ is entirely due to the effect of ions striking the cathode, with no allowance for a photon effect. Since this is the case, all calculations reported herein have completely ignored the transit time of the electrons, for reasons outlined elsewhere (ref 8).

Despite the above limitations, the agreement between the experimental data and the calculations is quite promising. As noted above, the calculated frequencies of relaxation oscillations are about one-sixth of that calculated using equation (1) with the calculation parameters, while the experimental measured values are about one-third of those calculated using equation (1) under the experimental conditions. This indicates an error of about a factor of about two between the calculations and the experimental data. A few exploratory calculations have shown that an assumption of 50 percent contributions to the secondary ionization coefficient from each of the ion component and the photon component is able to cut this error in about half. Further calculations will be necessary to verify this.

A more direct comparison can be made between the calculated and the experimental variation of frequency versus current. To make this comparison it is profitable to use similarity parameters, frequency/pressure, F/p, and current/(pressure)^2, I/p^2. Such a plot is shown in figure 19 for the calculated data shown in figure 6 (b) and the experimental data for one R_sC value taken from figure 17. The agreement of both the slope and intercept is satisfactory.

The variation of the LI product as a function of frequency, as shown in figure 9, shows surprising agreement with the measurements of Crawford (ref 9) in hot cathode mercury discharges at 1-μ pressure. Figure 3 of reference 9 shows that the measured LI product is 1.2×10^{-4} from 10 to 30 kc, then drops nearly linearly on a log-log plot to 1×10^{-5} at 1.8 Mc. This agreement is remarkable considering the dissimilarity of the gas, pressure, cathode mechanism, etc. The semicircular impedance locus, similar to that calculated and shown in figure 10, was also noted by Crawford (ref 9).

The voltage and current variation with time, calculated to simulate the 60-cps discharge and shown in figures 11 and 12, shows good agreement with the experimental data shown in figure 18 under comparable discharge conditions. The experimental data of El-Bakkal and Loeb (ref 10) taken in argon in glass cells also show complete qualitative agreement with the calculations of figures 11 and 12.

6. CONCLUSIONS AND FUTURE PROGRAM

It has been shown that the dynamic Townsend equations for continuity in a gas discharge with suitable boundary conditions and including space charge effects are able to explain relaxation oscillations in gas tube circuits. Although direct comparison with experimental measurements has not yet been accomplished, qualitative agreement is excellent and

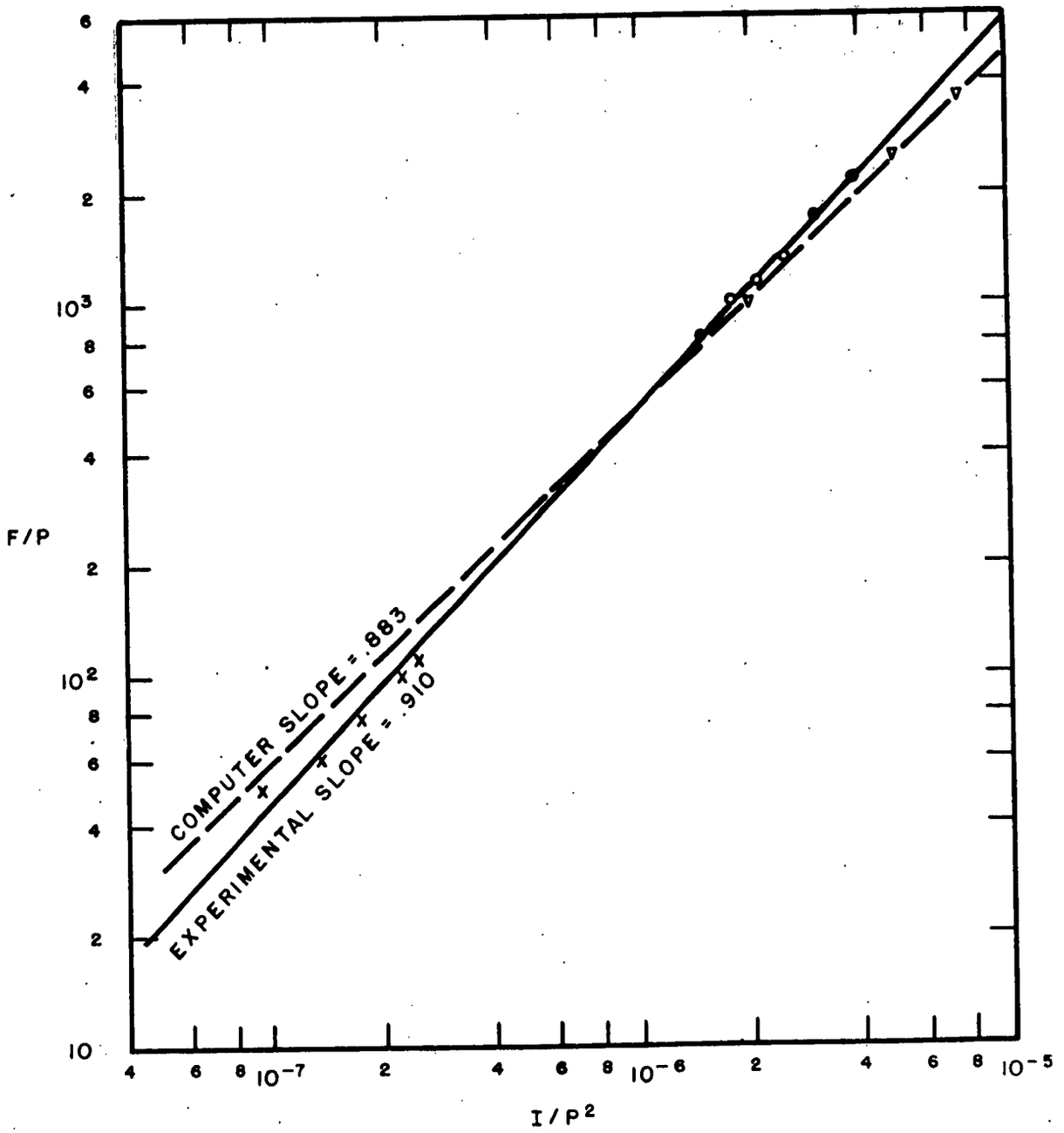

Figure 19. Comparison of computed frequency/pressure quotient variation with current-pressure squared quotient with measured values. Computer results for argon are shown as triangles, measured results in argon by crosses, and in hydrogen by circles.

the variation of frequency with current is in quantitative agreement.

It is planned to make further calculations to determine the effect of the variation of pressure, gap length, ionization coefficients, and a number of parameters peculiar to the computer program, upon the calculated relaxation oscillations. Further experimental work will be done whenever it seems feasible to check the calculations.

7. REFERENCES

(1) S. Seely, "Electron-Tube Circuits" McGraw-Hill, New York (1950) p 442 ff.

(2) D. J. Belknap, M. J. Reddan, and A. L. Ward, Bull. Am. Phys. Soc., II, 6, 392 (1961).

(3) A. L. Ward, Bull. Am. Phys. Soc. 7, 459 (1962).

(4) A. L. Ward, Bull. Am. Phys. Soc. 6 390 (1961), Proc. of the 5th Int. Conf. Ion. Phen. in Gases, North Holland Pub. Co., Amsterdam, 1961 p. 1595.

(5) A. L. Ward, L. G. Schneekloth, DOFL TR-1020, 30 March 1962.

(6) W. Kaufmann, Ann. der Physik 4, 158 (1900).

(7) A. L. Ward, Phys. Rev. 112, 1852 (1958).

(8) W. Börsch-Supan and H. Oser, J. Res., NBS, 67B, 41 (1963).

(9) F. W. Crawford, J. Appl. Phys. 33, 20 (1962).

(10) J. M. El-Bakkal and L. B. Loeb, J. Appl. Phys. 33, 1567 (1962).

APPENDIX—DERIVATION AND SOLUTIONS OF DIFFERENCE CURRENT EQUATION

The following definitions are made (see figure 1):

C : stray capacitance plus plate capacitance.

L_T: effective inductance of the tube.

R_t: instantaneous tube resistance (slope of the static characteristic).

R_s: series resistance.

V_o: maintaining voltage.

V_t: voltage across the tube.

I_T: current through the tube.

I_1: current through R_s.

I_2: current through C.

I_s: stationary current through tube.

When the tube is operating at a point on the static characteristic, a pure direct current is flowing or

$$I_2 = 0. \quad \text{Then } I_1 = I_T = I_s.$$

But at a point off the static characteristic, there will be current flowing through C, and therefore $I_1 = I_T + I_2$. Let us define a difference current $i_T = I_T - I_s$, and $i_1 = I_1 - I_s$. Thus we can say $i_1 = I_2 + i_T$.

The voltage drop across R_s plus the voltage drop across C must equal the supply voltage V_o:

$$R_s I_1 + \frac{1}{C} \int I_2 dt = V_o. \tag{1}$$

Since $i_1 = I_1 - I_s$, $R_s i_1 + R_s I_s + \frac{1}{C} \int I_2 dt = V_o$, or

$$R_s i_1 + \frac{1}{C} \int I_2 dt = V_o - R_s I_s \tag{2}$$

Also, the voltage drop across the tube must equal the voltage drop across C:

$$L_T \frac{dI_T}{dt} + R_T I_T = \frac{1}{C} \int I_2 dt \tag{3}$$

Since $i_T = I_T - I_s$,

$$L_T \frac{di_T}{dt} + R_T I_T + L_T \frac{dI_s}{dt} + R_T I_s = \frac{1}{C} \int I_2 dt \tag{4}$$

By definition, I_s is a constant; therefore, $dI_s/dt = 0$, and

$$L_T \frac{di_T}{dt} + R_T i_T + R_T I_s = \frac{1}{C} \int I_2 dt \tag{5}$$

Adding (2) and (5),

$$R_s I_2 + (R_s + R_T)\, i_T + L_T \frac{di_T}{dt} = V_o - (R_s + R_T) I_s \tag{6}$$

Differentiating equation (5) with respect to time t, we see that

$$I_2 = CL_T \frac{d^2 i_T}{dt^2} + CR_T \frac{di_T}{dt} \tag{7}$$

Substituting (7) into (6)

$$R_s L_T C \frac{d^2 i_T}{dt^2} + (L_T + R_s R_T) \frac{di_T}{dt} + (R_s + R_T) i_T = V_o - (R_s + R_T) I_s,$$

or

$$\frac{d^2 i_T}{dt^2} + \frac{L_T + R_s R_T}{R_s L_T C} \frac{di_T}{dt} + \frac{R_s + R_T}{R_s L_T C} i_T = V_o - (R_s + R_T) I_s. \tag{8}$$

$$= 0 \text{ by definition of } I_s.$$

This is the differential equation that must be solved. The fact that the equation has constant coefficients makes the solution and analysis much easier.

First, for convenience, let us make the following definitions and substitutions:

$$\lambda = -1/2\left(\frac{R_T}{L_T} + \frac{1}{R_s C}\right) \text{ and } \omega^2 = \left(1 + \frac{R_T}{R_s}\right) \frac{1}{L_T C} - \lambda^2 \tag{9}$$

Now the differential equation (8) becomes

$$\frac{d^2 i_T}{dt^2} - 2\lambda \frac{di_T}{dt} + (\omega^2 + \lambda^2) i_T = 0 \tag{10}$$

The general solution to (10) is

$$i_T = A \exp\{\lambda - (-\omega^2)^{1/2}\}t + B \exp\{\lambda + (-\omega^2)^{1/2}\}t \tag{11}$$

where A and B are arbitrary constants. To determine the characteristics of expression (11), it is necessary to examine the solution rather closely, keeping in mind the many possible values of the circuit components of figure 1.

Case I. $R_T > 0$

From the definition of λ in expression (9), we see that if R_T is a positive number, then λ is always negative.

A. ω^2 negative $\quad \left\{\lambda^2 > \left(1 + \frac{R_T}{R_s}\right) \frac{1}{L_T C}\right\}$

Under this condition, the exponentials in solution (11) are real. Therefore, the solution takes the form

$$\left(i_T = A_n \exp a_n t \qquad n = 1,2\right)$$

where $a_1 = \lambda - (-\omega^2)^{1/2}$ and $a_2 = \lambda + (-\omega^2)^{1/2}$, a_1 and a_2 always being negative numbers.

B. $\omega^2 = 0 \quad \left\{\lambda^2 = (1 + \frac{R_T}{R_s}) \frac{1}{L_T C}\right\}$

In this case there is a double root of the characteristic equation, that root being λ. Therefore, the general solution becomes

$$\left(i_T = (A + Bt) \exp \lambda t\right)$$

C. ω^2 positive $\quad \left\{\lambda^2 < (1 + \frac{R_T}{R_s}) \frac{1}{L_T C}\right\}$

Here the exponentials in (11) are imaginary. One form of the general solution is then

$$\left(i_T = A \exp (\lambda t) \sin (\omega t + B)\right.$$

This is an oscillating function in time with expontially decreasing amplitude.

Case II. $R_T = 0$

In this case, λ again is always negative, and the forms of the solution are the same as in Case I, except that the definitions of λ and ω become

$$\lambda = -\frac{1}{2R_s C} \text{ and } \omega^2 = \frac{1}{L_T C} - \lambda^2$$

Case III. $R_T < 0$

A. $\lambda = 0 \quad \{|R_T/L_T| = \frac{1}{R_s C}\}$

The differential equation (10) becomes

$$\frac{d^2 i_T}{dt^2} + \omega^2 i_T = 0$$

1. ω^2 negative $\quad \{|R_T| > R_s\}$

The solution is now real, taking the form

$$(i_T = A_n \exp \{\pm \omega t\}$$

2. ω^2 positive $\quad \{|R_T| < R_s\}$

The exponentials in (11) are imaginary, one form of the solution being

$$(i_T = A \sin (\omega t + B)$$

a constant-amplitude oscillation with frequency $\left(\frac{R_s + R_T}{R_s C L_T}\right)^{1/2}$

B. $\lambda < 0 \quad \{|\frac{R_T}{L_T}| < \frac{1}{R_s C}\}$

This case has the same form as Case I, since $\lambda < 0$.

C. $\lambda > 0 \quad \{|\frac{R_T}{L_T}| > \frac{1}{R_s C}\}$

1. $\omega^2 = 0 \quad \{\lambda^2 = \left(1 + \frac{R_T}{R_s}\right) \frac{1}{L_T C}\}$

Again the characteristic equation has a double root (λ), and the solution is

$$(i_T = (A + Bt) \exp \lambda t)$$

2. ω^2 positive $\left\{|R_T| < R_s\right\}$ and $\left(1 + \frac{R_T}{R_s}\right) \frac{1}{L_T C} > \lambda^2$

$$\left[(i_T = A \exp \lambda t \sin (\omega t + B)\right]$$

an oscillating current, with an exponentially rising amplitude.

3. ω^2 negative

ω^2 is negative (1) if $|R_T| > R_s$ or (2) if $|R_T| < R_s$ and $\lambda^2 \; |(1 + \frac{R_T}{R_s}) \frac{1}{L_T C}|$.

a. $|R_T| > R_s$

The solution takes the form,

$$i_T = A_n \exp a_n t, \text{ where } a_1 = \lambda + (-\omega^2)^{1/2} \text{ and } a_2 = \lambda - (-\omega^2)^{1/2}$$

which is an exponential function whose dominant term is an exponentially rising term.

b. $|R_T| < R_s$ and $\lambda^2 > |(1 + \frac{R_T}{R_s}) \quad \frac{1}{L_T C}|$

$i_T = A_n \exp a_n t$; both a_1 and a_2 are positive, so again we have an exponentially rising current.

Summary of Analysis

Oscillations occur if ω^2 is positive $\left[\text{if } \lambda^2 < \left(1 + \frac{R_T}{R_s}\right)\frac{1}{L_T C}\right]$

1. decreasing oscillation amplitude if $\lambda < 0$
2. increasing amplitude if $\lambda > 0$
3. constant amplitude if $\lambda = 0$

Exponentially varying current if $\omega^2 \leq 0$

1. decreasing exponential if $\lambda < 0$
2. increasing exponential if $\lambda > 0$
3. decreasing or increasing, depending on arbitrary constants, thus on inital conditions, if $\lambda = 0$

where $\lambda = -1/2\left(\frac{R_T}{L_T} + \frac{1}{R_s C}\right)$ and $\omega^2 = \left(1 + \frac{R_T}{R_s}\right)\frac{1}{L_T C} - \lambda^2$

DISTRIBUTION

Commanding General
U. S. Army Materiel Command
Washington, D. C.
Attn: AMCPP-CM-MI

Office of the Chief of Research & Development
Department of the Army
Washington 25, D. C.

Commanding Officer
Picatinny Arsenal
Dover, New Jersey
Attn: Tech Library

Commanding Officer
U.S. Army Research Office (Durham)
Box CM, Duke Station
Durham, North Carolina - 3 copies

Commander
U.S. Naval Ordnance Laboratory
White Oak, Silver Spring 19, Maryland
Attn: Tech Library

Department of the Navy
Bureau of Naval Weapons
Washington 25, D. C.
Attn: DLI-2, Tech Library

Commander
Naval Research Laboratory
Washington, D. C.
Attn: Tech Library

DDC Headquarters
Defense Documentation Center
Cameron Station Building No. 5
5010 Duke Street
Alexandria, Virginia
Attn: TISIA - 20 copies

National Bureau of Standards
Washington, D. C.
Attn: Library

DISTRIBUTION (Con't)

University of Michigan
Department of Electrical Engineering
Ann Arbor, Michigan
  Attn: Professor W. G. Dow

University of California
Department of Physics
Berkeley, California
  Attn: Professor L. B. Loeb

Thomas A. Edison Industries
Edison Laboratories
West Orange, New Jersey
  Attn: R. W. Crowe

Raytheon Manufacturing Company
Receiving Tube Division
55 Chapel Street
Newton 58, Massachusetts
  Attn: P. W. Stutsman

University of Minnesota
Dept of Physics
Minneapolis, Minnesota
  Attn: Professor H. J. Oskam

Bell Telephone Laboratories, Inc.
Murray Hill, New Jersey
  Attn: A. D. White/M. A. Townsend

Lockheed Missile and Space Co.
3251 Hanover
Palo Alto, California
  Attn: Dr. Leon Fisher

Minneapolis Honeywell Regulator Company
500 Washington Ave., South
Hopkins, Minnesota
  Attn: B. T. McClure

Sandia Corporation
Albuquerque, New Mexico
  Attn: G. W. McClure

DISTRIBUTION (Don't)

Microwave Laboratory
W. W. Hansen Laboratories of Physics
Stanford University
Stanford, California
Attn: Dr. F. W. Crawford

General Electric Company
Nela Park Laboratories
Cleveland, Ohio
Attn: Dr. Carl Kenty

INTERNAL DISTRIBUTION

Horton, B. M./McEvoy, R. W., Lt Col
Apstein, M./Gerwin, H. L./Guarino, P. A./Kalmus, H. P.
Schwenk, C. C.
Hardin, C. D., Lab 100
Sommer, H., Lab 200
Hatcher, R. D., Lab 300
Hoff, R. S., Lab 400
Nilson, H., Lab 500
Flyer, I. N., Lab 600
Campagna, J. H./Apolenis, C. J., Div 700
DeMasi, R., Div. 800
Landis, P. E., Lab 900
Seaton, J. W., 260
Van Trump, J. H., 930
Kaiser, Q. C., 920
Ward, A. L., 930 - 15 copies
Reddan, M. J., 930
Belknap, D. J., 930
Hershall, P., 930
Young, R. T., 320
Harris, F. T., 310
Rotkin, I./Godfrey, T. B./Eichberg, R. L.
Bryant, W. T./Distad, M. F./McCoskey, R. E./Moorehead, J.G.
Brenner, M., 723
Technical Information Office, 010 - 5 copies
HDL Library - 5 copies

Qualified requesters may obtain copies of this report from DDC
5010 Duke Street, Alexandria, Virginia

UNCLASSIFIED

AD________ Accession No._____

Harry Diamond Laboratories, Washington, D. C.

CALCULATIONS OF RELAXATION OSCILLATIONS IN GAS TUBE CIRCUITS
Alfred L. Ward, Larry G. Schneekloth

TR-1166, 26 August 1963, 19 pp text, 19 illus. DA-1A010501B010
AMCMS Code 5011.11.838, HDL Proj. #96600, UNCLASSIFIED report.

Temporal voltage-current dynamic characteristics have been computed using the Townsend continuity equations and Poisson's equation, with suitable initial and boundary conditions. In the current region of the negative static characteristic, small current perturbations initially grow exponentially in time if the external-circuit time constant is greater than the tube current-growth time constant. In a limited range of applied voltages, these oscillations become precisely repetitive in time, corresponding to the well known relaxation oscillations. The inductances and the negative resistances calculated from small-amplitude decaying oscillations agree precisely with those calculated using a sinusoidal incremental applied voltage of the same frequency and average current.

UNCLASSIFIED

1. Relaxation oscillations—Glow tubes
2. Glow discharges—Oscillations
3. Impedance calculations—Glow discharges
4. Glow tube circuits—Relaxation oscillations
5. Oscillation frequency—Current dependence

UNCLASSIFIED

AD________ Accession No._____

Harry Diamond Laboratories, Washington, D. C.

CALCULATIONS OF RELAXATION OSCILLATIONS IN GAS TUBE CIRCUITS
Alfred L. Ward, Larry G. Schneekloth

TR-1166, 26 August 1963, 19 pp text, 19 illus. DA-1A010501B010
AMCMS Code 5011.11.838, HDL Proj. #96600, UNCLASSIFIED report.

Temporal voltage-current dynamic characteristics have been computed using the Townsend continuity equations and Poisson's equation, with suitable initial and boundary conditions. In the current region of the negative static characteristic, small current perturbations initially grow exponentially in time if the external-circuit time constant is greater than the tube current-growth time constant. In a limited range of applied voltages, these oscillations become precisely repetitive in time, corresponding to the well known relaxation oscillations. The inductances and the negative resistances calculated from small-amplitude decaying oscillations agree precisely with those calculated using a sinusoidal incremental applied voltage of the same frequency and average current.

UNCLASSIFIED

1. Relaxation oscillations—Glow tubes
2. Glow discharges—Oscillations
3. Impedance calculations—Glow discharges
4. Glow tube circuits—Relaxation oscillations
5. Oscillation frequency—Current dependence

UNCLASSIFIED

AD________ Accession No._____

Harry Diamond Laboratories, Washington, D. C.

CALCULATIONS OF RELAXATION OSCILLATIONS IN GAS TUBE CIRCUITS
Alfred L. Ward, Larry G. Schneekloth

TR-1166, 26 August 1963, 19 pp text, 19 illus. DA-1A010501B010
AMCMS Code 5011.11.838, HDL Proj. #96600, UNCLASSIFIED report.

Temporal voltage-current dynamic characteristics have been computed using the Townsend continuity equations and Poisson's equation, with suitable initial and boundary conditions. In the current region of the negative static characteristic, small current perturbations initially grow exponentially in time if the external-circuit time constant is greater than the tube current-growth time constant. In a limited range of applied voltages, these oscillations become precisely repetitive in time, corresponding to the well known relaxation oscillations. The inductances and the negative resistances calculated from small-amplitude decaying oscillations agree precisely with those calculated using a sinusoidal incremental applied voltage of the same frequency and average current.

UNCLASSIFIED

1. Relaxation oscillations—Glow tubes
2. Glow discharges—Oscillations
3. Impedance calculations—Glow discharges
4. Glow tube circuits—Relaxation oscillations
5. Oscillation frequency—Current dependence

UNCLASSIFIED

AD________ Accession No._____

Harry Diamond Laboratories, Washington, D. C.

CALCULATIONS OF RELAXATION OSCILLATIONS IN GAS TUBE CIRCUITS
Alfred L. Ward, Larry G. Schneekloth

TR-1166, 26 August 1963, 19 pp text, 19 illus. DA-1A010501B010
AMCMS Code 5011.11.838, HDL Proj. #96600, UNCLASSIFIED report.

Temporal voltage-current dynamic characteristics have been computed using the Townsend continuity equations and Poisson's equation, with suitable initial and boundary conditions. In the current region of the negative static characteristic, small current perturbations initially grow exponentially in time if the external-circuit time constant is greater than the tube current-growth time constant. In a limited range of applied voltages, these oscillations become precisely repetitive in time, corresponding to the well known relaxation oscillations. The inductances and the negative resistances calculated from small-amplitude decaying oscillations agree precisely with those calculated using a sinusoidal incremental applied voltage of the same frequency and average current.

UNCLASSIFIED

1. Relaxation oscillations—Glow tubes
2. Glow discharges—Oscillations
3. Impedance calculations—Glow discharges
4. Glow tube circuits—Relaxation oscillations
5. Oscillation frequency—Current dependence

REMOVAL OF EACH CARD WILL BE NOTED ON INSIDE BACK COVER, AND REMOVED CARDS WILL BE TREATED AS REQUIRED BY THEIR SECURITY CLASSIFICATION.